Modeling Crosstalk Induced Delay

Chung-Kuan Tsai, Malgorzata Marek-Sadowska
University of California, Santa Barbara

Abstract

The amplitude of coupled noise is often used in estimating the crosstalk effect. Coupling noise-induced delay measures the impact of crosstalk on circuit performance. Efficient computation of worst case noise-induced delays are essential, because such calculations are performed a huge number of times during timing analysis. In this paper we analyze the problem of crosstalk noise-induced delay in one logic stage. We observe that the popular method of crosstalk delay computation based on superposition of the victim's switching waveform and the noise waveform determined when the victim is quiet, produces an underestimation of delay. To capture the crosstalk noise-induced delay, we introduce the concept of dynamic coupling noise waveform. We propose a method of synthesizing the dynamic noise waveform and using it to estimate the delay change.

1 Introduction

The delays of circuits manufactured in deep sub-micron technologies are dominated by interconnect delays. Additionally, wires tend to be tall and narrow, which implies that coupling capacitances dominate wire capacitances to ground. These effects make the coupling noise delays significant. Estimating the effect of coupling noise on delay is difficult, even for a single logic stage. Efficient computation of delay change due to coupling noises is therefore of interest.

Fig. 1(a) shows one stage of logic. Each wire is driven by a buffer, and connects to the driver of the next stage. There are self capacitances C_{gi} between wires and the ground below them, and coupling capacitances C_{ci} between any two adjacent wires.

When one wire is switching, its voltage level changes, thus the amount of electric charge accumulated on the coupling capacitance also changes. The amount of electrical charge change corresponds to the change of the adjacent wire's voltage level, constituting the *coupling noise*. Usually we call the wire which induces the coupling noise, the *aggressor*, and the wire which is subject to it, the *victim*.

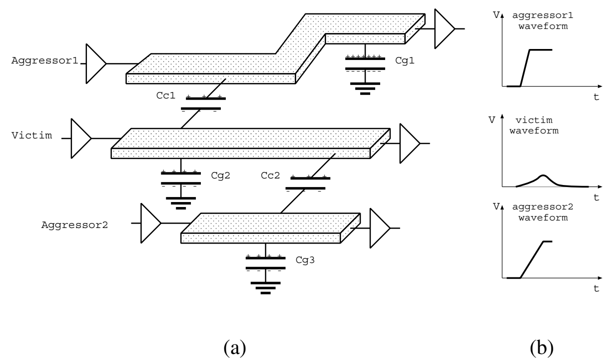

Figure 1. A typical one stage of interconnects. (a) A victim and its two aggressors. (b) Switching on the aggressors induces a noise on the victim.

The coupling noise on the quiet victim will be referred to as the *static noise*. For example, in Fig. 1(b), the middle waveform on the victim wire is the static coupling noise waveform.

When the victim and aggressors are switching, the coupling noise affects the victim transition waveform, and thus changes the victim's transition delay. For example, in Fig. 2(a), the victim is falling while the aggressor is rising. The victim drain current I_d is discharging the victim wire, while the aggressor is depositing more charge on it. Therefore the aggressor slows down the rate of the victim's wire charge reduction, and also slows down the drop rate of the victim's drain voltage. In Fig. 2(b), we show the waveform of the victim drain voltage V_d. We measure the wire delay from the time (t_0) when the rising transition of the victim gate achieves half of the voltage swing, to the time when the falling transition of the victim drain voltage reaches half of the voltage swing. We denote the latter time by t_1 if the victim's falling transition occurs with quiet aggressor, and t_2 if the aggressor is switching. Therefore the aggressor switching increases the victim delay by the amount of $t_2 - t_1$.

The aggressor's skew is defined as the aggressor's switching time relative to that of the victim's. It affects the slowdown and the skew-slowdown relationship between a victim and an aggressor is often of great interest.

Dartu et al. pioneered the method of evaluating the de-

0-7695-1881-8/03 $17.00 © 2003 IEEE

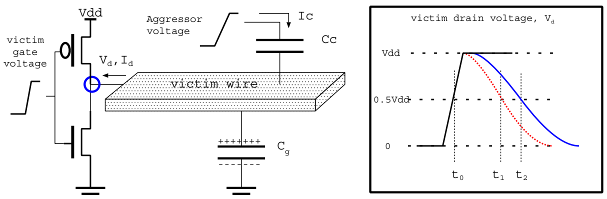

(a) (b)

Figure 2. The victim drain current I_d discharges electrical charge on the victim wire, while the aggressor deposits charge on the victim wire by I_c. Victim drain voltage waveform is plotted in the right block.

lay increase due to capacitive coupling by the waveform-based superposition[3]. This method consists of three steps. First we compute the static coupling noise waveform N_1 induced by the aggressor on the quiet victim. Second, we compute the noise-free victim transition waveform V. Third, N_1 and V waveforms are superposed together, and the delay is determined from the superposition waveform W_1. Fig. 3 illustrates those steps. This method is simple and easy to use. Many publications suggest approximate analytical models to evaluate the static noise N_1 and victim transiting V waveforms [1][4][8][9]. Sylvester et al. [7] use Dartu's method and analytical noise models, and in $0.25\mu m$-technology they observe some error in computing crosstalk induced delay increase. In more advanced technologies, the error of the combined waveform becomes greater. Sirichotiyakul et al. [6] reduce the error by modeling the transiting victim driver. Their method requires on-the-fly nonlinear simulations during gate modeling with cell-level analysis. Their approach to determine aggressor alignment is based on look-up tables with given victim slopes, noise pulse widths and heights. In this paper, we propose a modified noise model which can be used with Dartu's method [3] without non-linear simulations.

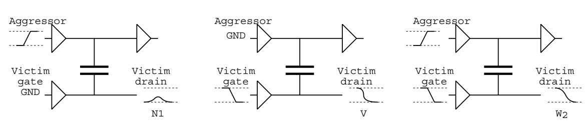

Figure 3. The excitation of static noise waveform N_1, victim transition waveform V and W_2.

Fig. 4 shows waveforms for an interconnect stage of two $100\mu m$-length wires fully coupled at minimum spacing in $70nm$-technology. The aggressor driver size is four times the minimum-size victim driver. The aggressor has a rising transition while the victim has a falling transition. N_1 and V waveforms in Fig. 4 are determined by SPICE for the conditions illustrated in Fig. 3. W_2 is the SPICE-obtained victim transition waveform when the aggressor is switching.

We define the *dynamic noise waveform* N_2 as the waveform the aggressor induces on the switching victim. The dynamic noise waveform can be viewed as a difference between the waveforms W_2 and V. The amount of slowdown estimated from the superposition method is the delay difference between V and W_1, which is $34ps$ in this particular case. However, the actual slowdown is $112ps$, which is the delay difference between V and W_2. This is because N_1 underestimates the dynamic noise waveform N_2. In order to benefit from the simple analysis structure of the superposition method, we propose a method of synthesizing the dynamic noise waveform N_2.

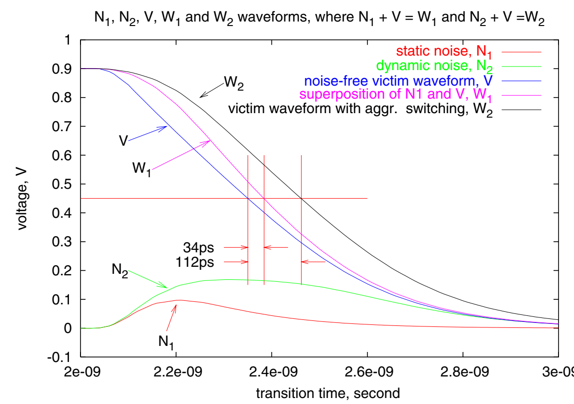

Figure 4. The SPICE simulation obtained noise and transition waveforms.

When there are multiple adjacent aggressors switching in the opposite direction to the victim, then the joint slowdown needs to be considered. The conventional method estimates the maximum joint slowdown by directly adding up the maximum slowdowns of all aggressors. This is shown by Sasaki et al. [5] to be an overestimation. Sasaki et al. have developed a relative window analysis method, which excludes unrealizable cases when the victim needs to switch at different times to suffer from the maximum slowdown of each aggressor. They determine each aggressor's slowdown with respect to the victim signal arrival time, and add the slowdowns. The slowdown is considered as a function of the victim signal arrival time.

In some cases, directly adding up each aggressor's slowdown results in error. See for example, Fig. 5. We denote the noise with skew $\phi = 100ps$ as N_{100}, and the noise with skew $\phi = 300ps$ as N_{300}. We observe that N_{300} alone doesn't cause any slowdown, because N_{300} only affects the portion of the victim waveform below $0.5V_{dd}$. However, with the presence of N_{100} noise, the joint slowdown of N_{100} and N_{300} is almost twice the slowdown from N_{100} alone. Therefore, the only way to accurately estimate the amount of slowdown is to evaluate the victim waveform subject to

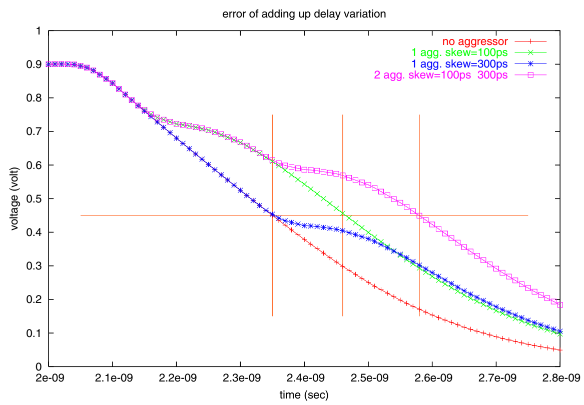

Figure 5. The victim waveforms. From bottom up: noise-free V, with 1 aggressor skew $\phi = 300ps$, with 1 aggressor skew $\phi = 100ps$, and with 2 aggressors $\phi_1 = 100ps, \phi_2 = 300ps$.

both noises, instead of to each noise individually.

A different approach has been proposed in [2], where the authors address the aggressor alignment problem for the worst case delay and use it in transistor-level simulation engine.

The paper is organized as follows. In Section 2 we analyze and model the dynamic noise N_2. In Section 3 we propose a methodology to synthesize the dynamic noise waveform. In Section 4 we present the experimental results. We conclude this paper in Section 5.

2 The Dynamic Noise Waveform N_2

We represent the delay slowdown by τ, the skew between the victim and aggressor by ϕ, and the absolute time by t. The waveform of the dynamic noise N_2, which is imposed by an aggressor on a transiting victim, is plotted in Fig. 6. The aggressor skew is swept from $-0.6ns$ to $0.8ns$. In Fig. 6 we also show the victim transition waveform for reference. The dynamic noise amplitude and width depend on aggressor skew. The circuit we consider consists of two fully coupled $100\mu m$ metal wires with minimum spacing, and the aggressor driver size is four times the minimum size of the victim. The feature size is $70nm$.

When we shift the noise by the amount of its aggressor skew, as in Fig. 7, we observe that the dynamic noise waveforms N_2 are all of greater size in terms of the amplitude and width than N_1, and all the N_2 waveforms with positive skew have similar shapes. Moreover, the size of N_2 waveform approaches that of N_1 as the aggressor skew approaches positive or negative infinity.

To investigate the reason that the size of N_2 is greater than that of N_1, we look at the victim transition trajectory, the victim drain current I_d as a function of the victim drain

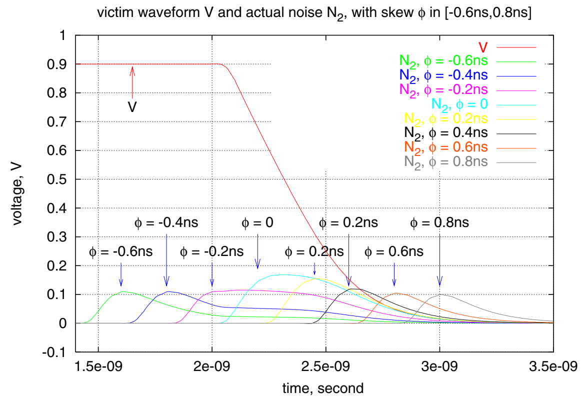

Figure 6. The victim transition waveform V and the dynamic noise waveforms N_2 for the skew ϕ ranges from $-0.6ns$ to $0.8ns$.

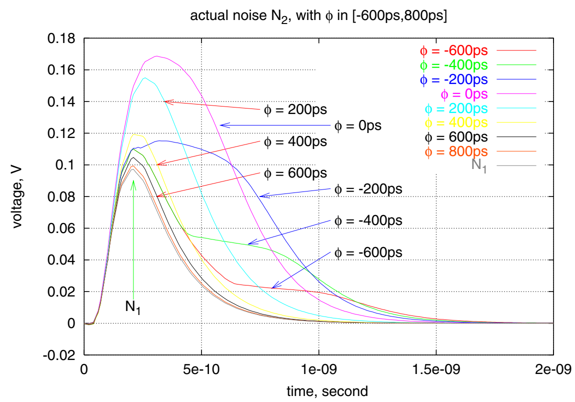

Figure 7. The dynamic noise N_2 waveforms, with skew $\phi \in [-400ps, 500ps]$.

voltage V_d. See Fig. 8.

When the N_1 noise is generated, the victim doesn't switch, and the victim gate terminal is fixed at V_{dd}. The noise changes the drain voltage, and because the victim `nMOS` is in its linear region, the drain voltage V_d linearly corresponds to the drain current I_d. Therefore, we can substitute the `nMOS` by an equivalent resistance corresponding to the $V_d - I_d$ slope. This is the reason that we can substitute the non-switching transistors by their equivalent resistance and still maintain high accuracy.

However, when the victim and the aggressor are both switching, the victim transition trajectory is very close to the trajectory of the V waveform, in which case the aggressor doesn't switch. When the transition delay is calculated, only the portion of the victim transition waveform which is above $0.5V_{dd}$ is of interest. For that portion of waveform, the victim drain voltage is always greater than $0.5V_{dd}$, which means that the victim `nMOS` is in its saturation region. That is to say, when the victim is switching and the noise is present, the victim's `nMOS` acts more like a vary-

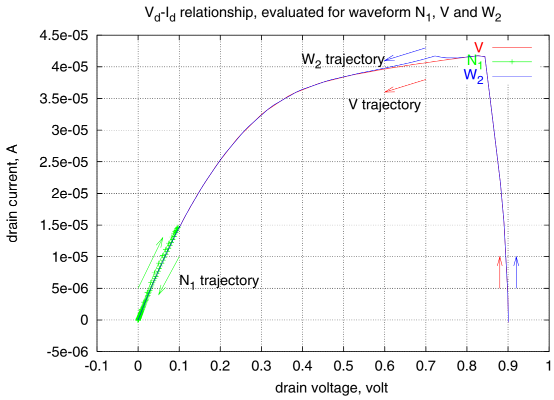

Figure 8. The victim transition trajectory. In the N_1 case, the $V_d - I_d$ is confined within the segment of $[0, 0.1V]$. When both aggressor and victim are switching, the victim transition trajectory does not differ much from the case when only the victim is switching.

ing current source than a resistance. However, this varying current source is a function of V_d and of the noise arrival time. Therefore, the value of the current source needs to be calculated according to the dynamic noise magnitude and noise arrival time. This process is very time-consuming and thus infeasible. To model the dynamic noise waveform N_2 accurately we need a different approach.

3 Synthesizing the Dynamic Noise

Here we assume that the dynamic noise waveform caused by one aggressor is independent from other aggressors. Therefore we can compute independently dynamic noise waveforms caused by each aggressor on the victim. Then we add up the noises and the victim transition waveform applying superposition and estimate the slowdown.

3.1 Sensitive Region

The *Sensitive Region* is the range of aggressor skew over which the coupling noise affects the victim's transition. It is calculated from the range of the static coupling noise and the range of the victim transition. We define the range of static noise as the absolute time over which its amplitude is greater than 10% of the peak amplitude. Further, the range of the victim transition waveform is defined as the time when the transition waveform has amplitude between 90% and 10% of V_{dd} (assuming victim has voltage swing V_{dd}). The range of the noise is $[t_1, t_2]$, and the range of the transition is $[t_3, t_4]$, where $t_1 < t_2$ and $t_3 < t_4$. Please note that there is no constraint between $[t_1, t_2]$ and $[t_3, t_4]$. The sensitive region is then $[\phi_1, \phi_2]$, where $\phi_1 = t_3 - t_2$ and $\phi_2 = t_4 - t_1$. When the skew is less than $t_3 - t_2$, the noise range is earlier than $[t_1 + t_3 - t_2, t_2 + t_3 - t_2] = [t_3 - (t_2 - t_1), t_3]$, and the noise doesn't affect the victim transition. Similarly, if the skew is greater than $t_4 - t_1$, then the noise range is later than t_4; thus the noise cannot affect the victim transition either.

3.2 Dynamic Noise Ratio

When the aggressor switches in the sensitive region, the dynamic coupling noise N_2 is different from the static noise N_1. To characterize the N_2 waveform efficiently, we assume that the N_2 waveform is geometrically similar to the static noise waveform N_1. Therefore as long as we can find the dynamic noise ratio λ of N_2 over N_1, we can determine the N_2 waveform by simply scaling the N_1 waveform by the ratio λ.

3.3 Maximum Dynamic Noise Amplitude

We define τ_1 as the maximum slowdown caused by the static noise N_1, and τ_2 as the maximum slowdown caused by dynamic noise. $\max(N_1)$ and $\max(N_2)$ are the maximum noise amplitudes of noise N_1 and N_2. We assume that the maximum slowdown caused by the dynamic (static) noise is proportional to the maximum amplitude of the dynamic (static) noise. That is to say

$$\frac{\tau_2}{\tau_1} \approx \frac{\max(N_2)}{\max(N_1)} = \lambda. \tag{1}$$

The maximum slowdown caused by dynamic noise τ_2 will be evaluated below. Therefore the maximum amplitude of the dynamic noise, $\max(N_2)$, can be calculated from (1).

Claim. When the aggressor's voltage is rising and the victim's is falling, the maximum slowdown τ_2 is $C_c V_{dd}/I_{dm}$, where I_{dm} is the victim drain current I_d when the victim is biased at $V_d = 0.5V_{dd}$, $V_g = V_{dd}$.

Proof. Let the aggressor voltage swing be V_{dd}, and the coupling capacitance of that aggressor be C_c. The aggressor induces electric charge on the victim in the amount of $Q = C_c V_{dd}$. Only the noise which is induced on the upper half of the victim transition waveform (the portion above $0.5V_{dd}$) is of interest. The minimum drain current corresponding to that portion of waveform is therefore I_{dm}, the one evaluated at $V_d = 0.5V_{dd}$. The upper half victim transition waveform corresponds to the victim nMOS saturation region. Therefore the nMOS acts like a current source with current magnitude $I(t)$, where $I(t) \geq I_{dm}$.

The amount of time for $I(t)$ to dissipate the total charge Q is $Q/I(t)$. This is the upper bound of slowdown caused by the aggressor because in reality $I(t)$ may keep dissipating the charge after the victim waveform falls below $0.5V_{dd}$. In terms of mathematical equations, we have

$$\tau_2 = \int_{\text{noise range}} 1 \cdot dt = \int d\frac{q}{I(t)} \leq \int \frac{dq}{I_{dm}} = \frac{Q}{I_{dm}}.$$

Therefore the maximum slowdown τ_2 caused by dynamic noise is bounded by Q/I_{dm}, where $Q = C_c V_{dd}$. $\square$

3.4 Dynamic Noise Ratio as a Function of Aggressor Skew

When the aggressor skew is within the sensitive region, the dynamic noise ratio λ is a function of aggressor skew ϕ. The maximum value of $\lambda(\phi)$ is given in Section 3.3. To simplify the analysis, we assume that $\lambda(\phi)$ is a triangular function. To find the value of the skew ϕ over which $\max(\lambda)$ occurs is not trivial. For now, to keep the analysis simple, we assume that $\max(\lambda)$ is at ϕ_m, which is the skew at which the static noise N_1 causes the maximum slowdown of the victim transition (Fig. 9).

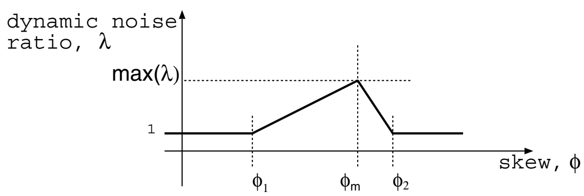

Figure 9. The triangular $\lambda(\phi)$ function is determined at three points: $(\phi_1, 1)$, $(\phi_2, 1)$ and $(\phi_m, \max(\lambda))$.

When multiple aggressors induce noises onto the victim, we synthesize each dynamic noise waveform by scaling each static noise waveform according to $\lambda(\phi)$. Then we superpose the dynamic noise waveforms onto the victim transition waveform and obtain the composite noise waveform. The slowdown is calculated from the composite waveform.

4 Experimental Results

The first experiment is for two $100\mu m$ metal wires fully coupled, similarly to those in the previous examples. Fig. 10(a) shows the results when the aggressor driver size is minimal, the same as the victim's. In this case, our method overestimates the slowdown. However, when the aggressor size is three times that of the victim, as in Fig. 10(b), the actual maximum slowdown ($117ps$) is very close to the estimated ($127ps$) slowdown. Fig. 11 shows slowdown as functions of the victim input transition time. We observe that our method overestimates the slowdown when the aggressor driver size is minimal, the same as the victim's in Fig. 11(a). When the aggressor driver is three times that of the minimum-size victim driver in Fig. 11(b), our method provides a good approximation of SPICE simulation results.

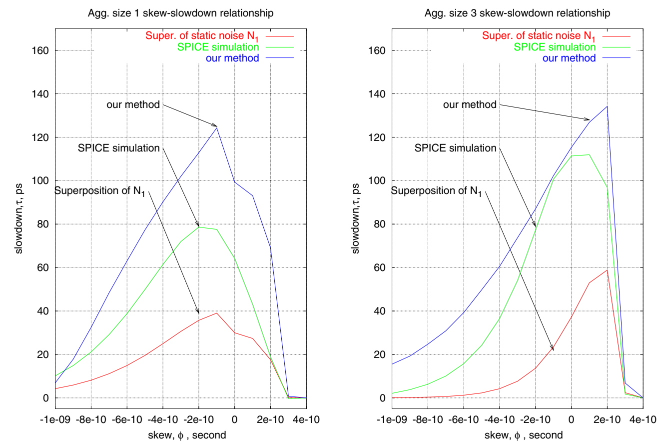

(a) Aggressor size 1 (b) Aggressor size 3

Figure 10. The skew-slowdown relationship for different aggressor sizes.

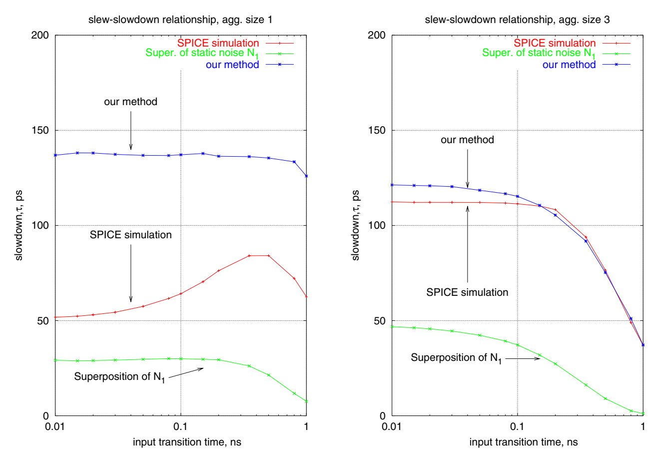

(a) Aggressor size 1 (b) Aggressor size 3

Figure 11. The slew-slowdown relationship for different aggressor sizes.

The second experiment is for three $100\mu m$ metal wires coupled on full length, with the victim in the center and two adjacent aggressor wires. With the first aggressor switching at zero skew, we can see the skew-slowdown relationship of the second aggressor. In Fig. 12(a), the two aggressors are the same size as the victim; our method overestimates the slowdown. However, in Fig. 12(b), when the aggressor driver size is three times that of the victim, our method can estimate the slowdown very accurately.

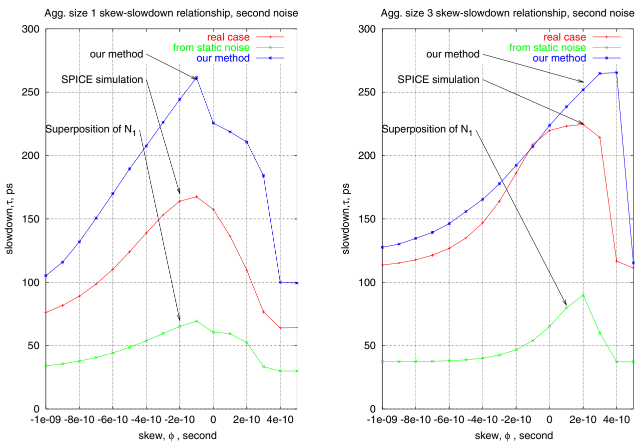

(a) Aggressor size 1 (b) Aggressor size 3

Figure 12. The skew-slowdown relationship for different aggressor sizes.

The slowdown is also a function of wire length. Let two wires of the same length be capacitively coupled, and the aggressor skew be zero. The length-slowdown relationship is shown in Fig. 13. In Fig. 13(a) the aggressor driver size is the same as that of the victim. We observe that our method as before overestimates the slowdown. However, when the aggressor size is three times that of the victim, as in Fig. 13(b), our method fits the `SPICE` simulation very well.

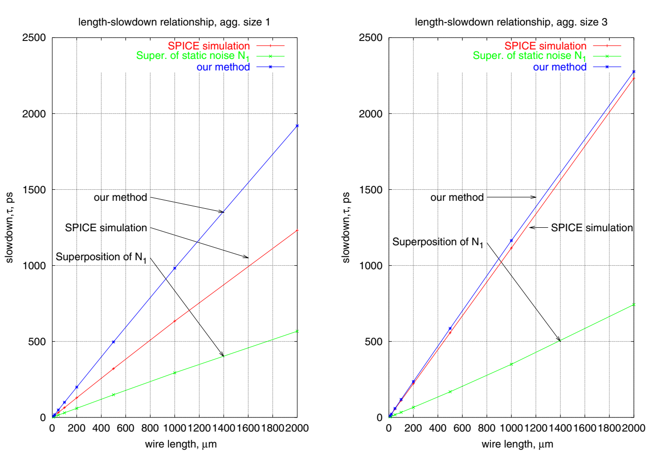

(a) Aggressor size 1 (b) Aggressor size 3

Figure 13. The length-slowdown relationship for different aggressor sizes.

5 Conclusion and Future Work

In this paper, we studied the coupling noise-induced delay slowdown as a function of the aggressor's skew. We introduced the concept of dynamic coupling noise, and we proposed an approach to synthesize its waveform. By superposing this dynamic noise waveform with the victim transition waveform, we estimated the slowdown with respect to the aggressor's skew. When the coupling noise is large, or there are multiple coupling noises, our method estimates the slowdown very well. Moreover, when the coupling noise is small, our method gives an upper bound of the slowdown.

Our experimental results suggest that the computation of maximum slowdown in aligning dynamic noises is not trivial. Also, the mechanism of delay speedup differs from that of the slowdown. Therefore, further analysis is needed for the combined effect of delay speedup and slowdown. Our future work includes techniques to compute the maximum slowdown in the presence of multiple dynamic noises, and methods to estimate the combination of speedup and slowdown with respect to the aggressor's skews.

6 Acknowledgement

This work was supported by the National Science Foundation through grant CCR 0095069.

References

[1] E. Acar, F. Dartu, and L. Pileggi. TETA: Transistor-level waveform evaluation for timing analysis. *IEEE Transactions on Computer-Aided Design*, 21(5):650–616, May 2002.

[2] S. H. Choi, F. Dartu, and K. Roy. Timed pattern generation for noise-on-delay calculation. *Design Automation Conf.*, pages 870–873, 2002.

[3] F. Dartu and L. T. Pileggi. Calculating worst-case gate delays due to dominant capacitance coupling. *Design Automation Conf.*, pages 46–51, 1997.

[4] M. Kuhlmann and S. Sapatnekar. Exact & efficient crosstalk estimation. *IEEE Transactions on Computer-Aided Design*, 20(7):858–866, July 2001.

[5] Y. Sasaki and K. Yano. Multi-aggressor relative window method for timing analysis including crosstalk delay degradation. *IEEE Custom IC Conf.*, pages 495–498, 2000.

[6] S. Sirichotiyakul, D. Blaauw, C. Oh, R. Levy, V. Zolotov, and J. Zuo. Driver modeling and alignment for worst-case delay noise. *Design Automation Conf.*, pages 720–725, 2001.

[7] D. Sylvester and C. Hu. Analytical modeling and characterization of deep-submicrometer interconnect. *IEEE Proceedings*, pages 634–664, May 2001.

[8] S. Wong, G. Lee, and G. Ma. Modeling of interconnect capacitance, delay & crosstalk in VLSI. *IEEE Transactions on Semiconductor Manufacturing*, 13(1):108–111, February 2000.

[9] Q. Yu and E. Kuh. Moment computation of lumped & distributed coupled rc trees with application to delay & crosstalk estimation. *IEEE Proceedings*, 89(5):772–788, May 2001.